

The universal density profile of the central region of dark matter haloes

A. N. Baushev

DESY, 15738 Zeuthen, Germany

Institut für Physik und Astronomie, Universität Potsdam, 14476 Potsdam-Golm, Germany

ABSTRACT

We consider the density profile of the central region of dark matter haloes. It turns out that under very general conditions the profile is universal: it depends almost not at all on the properties of the initial perturbation and is very akin, but not identical, to the Einasto profile.

We estimate the size of the ‘central core’ of the distribution, i.e., the extent of the very central region with a respectively gentle profile, and show that the cusp formation is unlikely, even if the dark matter is cold. We also indicate that the density profile of the outer part ($r > 0.5R_{vir}$) of the haloes significantly depends on the initial conditions and should not be universal, in contrast to the central area. All these results can be useful both to indirect search of the dark matter and to N-body simulations of the structure formation.

Key words: cosmology: dark matter, cosmology: large-scale structure of Universe, elementary particles, methods: analytical.

1 INTRODUCTION

The problem of the Universe structure formation is still far from the complete solution. Since the task is essentially non-linear, N-body simulation is one of the possible ways to solve it. An exceptional result found in the simulations is that extremely varied initial density profiles evolve very soon into a very similar ‘universal’ density profile (hereafter UDP). The UDP closely resembles the Navarro-Frenk-White profile (Navarro, Frenk, & White 1997), though further simulations show (Moore, Lake, & Katz 1998; Gao et al. 2008; Diemand et al. 2008; Stadel et al. 2009; Navarro et al. 2010) that it is closer to the Einasto one (Einasto 1969), i.e., the density in the very centre of the halo tends to a constant value instead of behave as r^{-1} .

The reasons of the universal density profile appearance are still unclear. It seems likely that the presence or absence of substructures is not determinative for the process: the UDP appears, even if we consider a halo collapse with no substructures (Huss, Jain, & Steinmetz 1999) or hot dark matter haloes (Wang & White 2009). Of course, N-body simulations are not infallible: in particular, they model minuscule dark matter particles by $10^4 - 10^6 M_\odot$ bodies. Contrary to the particles, the bodies can scatter on large angles during close approaches, and in order to avoid this effect, the newtonian potential of test bodies is modified. However, the N-body simulations excellently describe observed properties of galaxy clusters; in particular, their density profiles

are close to the UDP. Therefore the modelling results are adequate, at least, in the important case of the highest mass systems, which indicates that the universal density profile is not a calculational artefact and has some physical motivation (Dalal, Lithwick, & Kuhlen 2010).

It is interesting to note, however, that if we consider a scale-free initial profile, UDP often does not appear, and the final profile depend on the initial one (Lithwick & Dalal 2011). We should mention that such profiles cannot describe the structure formation in the real Universe, where there is always some characteristic initial radius \mathfrak{R} of the region, from which the majority of the particles will be captured by the forming halo, while the matter outside of \mathfrak{R} will be captured by the other nearby structures or form a diffuse component. As we will see below, the existence of characteristic scale \mathfrak{R} of the initial profile plays an important role in the UDP formation.

We do not try to fully explain the origin of the universal density profile in this letter. We shall show, however, that under some very general conditions, the central part of the formed halo should really have almost the same density profile, close, but not equal, to the Einasto one.

2 ENERGY SPECTRUM

In order to explain some properties of the distribution of real systems, the ‘violent relaxation’ is frequently in-

volved, i.e. the intensive energy exchange between dark matter particles at the initial stage of the collapse, when strong small-scale gravitational fields occur in the centre part of the halo (Lynden-Bell 1967). Further investigations showed, however, that the situation is more likely quite the contrary: the energy of the majority of the particles remains quite close to the initial one (Quinn & Zurek 1988; Zaroubi, Naim, & Hoffman 1996). It is the fact that we take as the starting point: it means that the final energy distribution of the particles is respectively close to the initial one.

Let us consider the initial distribution of matter. Hereafter in this article we will consider a spherically-symmetric task and neglect the presence of baryon matter. The mass and initial radius of the halo are m and \mathfrak{R} . Let us denote by $\epsilon = \frac{v^2}{2} + \phi$ the total energy of a unit mass of the matter, ϕ is the gravitational potential. If the dark matter is cold, the initial velocity of the matter may be thought of as to be zero without loss of generality (Gorburnov & Rubakov 2011). (As we will see at the end, the conclusions of this section is also valid for the warm dark matter). To begin with, let us consider the case when the matter is uniformly distributed inside \mathfrak{R} ($\rho = \text{const}$, the Tolman case). Inside the sphere:

$$\phi(r) = \frac{Gm}{\mathfrak{R}} \left(\frac{3}{2} - \frac{1}{2} \left(\frac{r}{\mathfrak{R}} \right)^2 \right) \quad (1)$$

$$dm = \frac{1}{3} \frac{m}{\mathfrak{R}} \left(\frac{r}{\mathfrak{R}} \right)^2 dr \quad (2)$$

Hence we obtain the initial energy distribution of the substance:

$$\frac{dm}{d\epsilon} = \left(\frac{3\mathfrak{R}}{G} \right) \sqrt{3 + \frac{2\epsilon}{\Phi}}; \quad \epsilon \in \left[-\frac{3}{2}\Phi; -\Phi \right] \quad (3)$$

where $\Phi \equiv \frac{GM}{\mathfrak{R}}$. Performing similar calculations, we obtain for the case of initial density perturbation $\rho \propto r^{-1}$

$$\frac{dm}{d\epsilon} = \frac{2m}{\Phi} \left(2 + \frac{\epsilon}{\Phi} \right); \quad \epsilon \in [-2\Phi; -\Phi] \quad (4)$$

and for initial profile $\rho \propto r^{-2}$

$$\frac{dm}{d\epsilon} = \frac{m}{\Phi} \exp \left(1 + \frac{\epsilon}{\Phi} \right); \quad \epsilon \in [-\infty; -\Phi] \quad (5)$$

As one can see in Fig. 1, distributions (3), (4), and even (5) differ not so strongly.

It seems reasonable to say that the initial energy distribution is similar to (3) under any reasonable choice of shape of the initial perturbations. Indeed, a real (smooth) density perturbation collapses when $\frac{\delta\rho}{\rho} = \beta \simeq 1$, and β weakly depends on the shape of the initial perturbations. Consequently, if the initial shape of $\delta\rho(r)$ is a smooth function, distributions of ϕ and dm differs from (1) and (2) only on a multiplier of the order of 2. Consequently, distribution $dm/d\epsilon$ does not differ very significantly from the uniform one (3). Second, if we divide a spherically symmetric initial distribution on radial layers of thickness dr , ϵ is constant within the layer, and the volume of the layer grows as $\left(\frac{r}{\mathfrak{R}} \right)^2$. As a result, the particles with $\epsilon \simeq -\Phi$ (which corresponds to $r = \mathfrak{R}$) dominate in the initial energy spectrum even in the case of quite a steep profile ($\delta\rho \sim r^{-1}$). A strong departure from (3) will take place only if the initial profile is very steep (for instance, $\delta\rho \sim r^{-3}$). On the other hand, such profiles are hardly suitable to describe the initial perturbations of the dark matter.

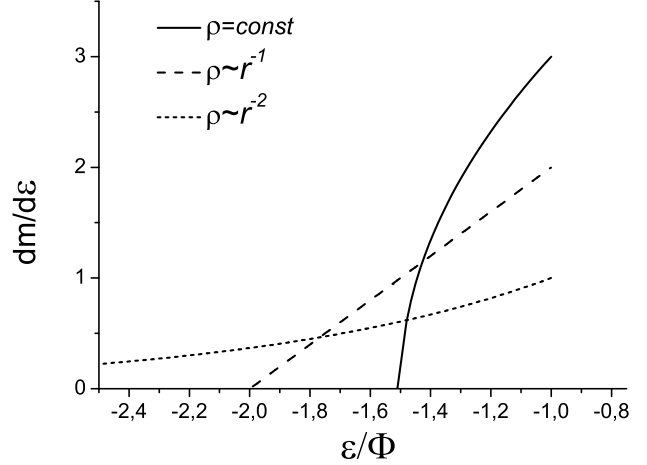


Figure 1. Energy spectra $\frac{dm}{d\epsilon}$ for various forms of initial perturbations. Apparently, there are no particles with $\epsilon > -\Phi$.

So for a large variety of initial conditions the initial energy distribution of the particles is similar to (3), at least, in the following sense: the majority of the particles have the energy close to $-\Phi$, and their energy distribution is quite narrow. In case of distribution (3), for instance, for all the particles $\epsilon \in [-\frac{3}{2}\Phi; -\Phi]$. This conclusion is also valid for the warm dark matter. Indeed, the smearing of the energy spectrum with respect to the cold dark matter case is of the order of the temperature of dark matter at the moment of the structure collapse. For the structure to be able to collapse, the temperature should be much lower than Φ .

As we have already mentioned, the energy distribution of the particles changes quite weakly with respect to the initial one. Therefore, the similarity between the initial distributions leads to the similarity of the particle energy spectra of the relaxed halo. But how can the system evolve at all, if the energies of the bulk of the particles remain almost the same? The mechanism is the following: the particles oscillate in the potential well. Initially they oscillate cophasal. Then, even if the energies of the particles remain constant, their phases diverge. Typically, the period sharply depends on ϵ for the majority of potential wells. But even if the energies of the particles precisely coincide, their phases can diverge as a result of a small nonsphericalness, perturbations from the nearby structures etc. Finally, the phases of the oscillations are mixed thoroughly, and each phase becomes equiprobable. This is exactly the situation, corresponding to the stationary halo. It is important to underline that the phase mixing goes on continuously, in contrast to the energy exchange, which is effective only during the first short stage of violent relaxation.

It is significant that the small energy evolution of the majority of the particles is not only an effect discovered by N-body simulations, but it has deep physical reasons. As we could see, the main fraction of mass of the future halo is initially concentrated in the outer layers with the highest initial r (since their volume grows as $(r/\mathfrak{R})^2$). Meanwhile, as it was shown by Lynden-Bell (1967), the efficiency of all relaxation processes (and so the alternation of the particle energy) rapidly drops with r : even in that work the outer part of the system remained unrelaxed.

However, the strongest argument in favour of the energy spectrum conservation during the relaxation is the existence of the standard density profile itself. Indeed, let us suppose that a strong energy trade between dark matter particles occurs. Then the energy exchange can appear only on the initial stage of the halo formation: the energy exchange is implemented by the variable small-scale gravitational fields appearing only just after the halo collapse. It is apparent, however, that in this case the energy trade strongly depends on the initial conditions. Indeed, if the initial perturbation is flat (above-mentioned Tolman case (3)), all the particles fall on the centre simultaneously. On the contrary, in the case of $\rho \sim r^{-1}$ or $\rho \sim r^{-2}$ initial profiles the outer particles fall on the centre much later, than the inner ones. Moreover, as long as the outer particles fall to the centre, the inner ones have already oscillated many times. So when the outer dark matter passes through the central region the first time, the region has already relaxed. It is clear that the conditions of the energy trade are completely different in this two cases, and if the density profile is defined by the energy redistribution, we might expect that the final density profiles were completely different. Since even though the final density profiles are similar, it means that the influence of the energy redistribution is not principle.

3 DENSITY PROFILE

Finally, the halo collapse forms stationary potential well $\phi(r)$. Each particle can be characterized by maximum radius r_0 the particle moves from the centre. As we could see (3), the initial energies of the particles are close, and the energy distribution does not change much during the relaxation. Consequently, r_0 of the majority of the particles are concentrated in a fairly narrow interval below some characteristic radius R (R is comparable, but does not obligatory coincide with \mathfrak{R}). The fractions of the halo mass formed by particles with $r_0 > R$ or $r_0 \ll R$ are small. It follows that $R \simeq R_{vir}$.

On the other hand, it means that the main contribution to the density in the central part of the halo is made by the particles that come there from the outside. Indeed, a formed halo has

$$k \equiv |(\phi(R_{vir}) - \phi(0))/\phi(R_{vir}) - \phi(\infty))| > 1$$

For instance, the Navarro-Frenk-White halo has $k = c_{vir}/\ln(c_{vir} + 1) - 1$, i.e. $k = 1.5$ even if $c_{vir} = 3$ (Baushev 2012). Comparing this with distribution (3), we may conclude that the majority of the particles has $r_0 > 0.5R_{vir}$. Of course, the real distribution differs from (3), and there are always some particles, which energies have completely changed, and their $r_0 < 0.5R_{vir}$. However, more than the half of the halo mass is typically concentrated inside $r = 0.5R_{vir}$, and if the particles with $r_0 < 0.5R_{vir}$ dominated there, it would mean that the energies of approximately the half of the halo particles have changed several times with respect to the initial ones, which is highly improbable, as we could see.

We can easily find the density distribution in the centre of the halo, created by the particles coming to this region from the outside. Let us single out the particles with a certain r_0 . We denote their total mass by m . According to

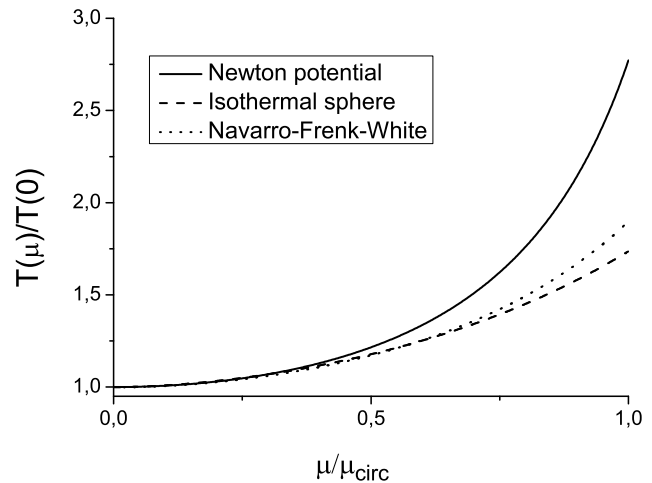


Figure 2. Ratios $T(\mu)/T(0)$ for the newtonian potential $\phi \propto -1/r$ (solid line), isothermal sphere $\phi \propto \ln(r)$ (dashed line) and Navarro-Frenk-White profile with $c_{vir} = 5$ (dotted line). The normalization of the potentials is chosen so that the mass inside r_0 is the same for all three cases. μ_{circ} corresponds to the circular orbit.

results of the numerical simulations, we assume that their specific angular momentum $\mu \equiv [\vec{v} \times \vec{r}]$ has Gaussian distribution

$$dm = m \frac{2\mu}{\alpha^2} \exp\left(-\frac{\mu^2}{\alpha^2}\right) d\mu \quad (6)$$

A particle moving in gravitational field $\phi(r)$ has two integrals of motion: μ and $\epsilon = \frac{v_r^2}{2} + \frac{\mu^2}{2r^2} + \phi$. The radial velocity of the particle is equal to

$$v_r = \sqrt{2(\phi(r_0) - \phi(r)) - \mu^2 \left(\frac{1}{r^2} - \frac{1}{r_0^2}\right)} \quad (7)$$

We introduce the maximum angular momentum of a particle wherewith it can reach radius r

$$\mu_{max}^2 = 2(\phi(r_0) - \phi(r)) \left(\frac{1}{r^2} - \frac{1}{r_0^2}\right)^{-1} \quad (8)$$

Then (7) may be rewritten as

$$v_r = \frac{\sqrt{r_0^2 - r^2}}{rr_0} \sqrt{\mu_{max}^2 - \mu^2} \quad (9)$$

A particle having maximal radius r_0 and minimal radius r_{min} contributes into the halo density on all the interval $[r_{min}, r_0]$. The contribution of a single particle of mass m on an interval dr is proportional to the time the particle passes on this interval (Baushev 2011).

$$\frac{dm}{m} = \frac{dt}{T} = \frac{dr}{v_r T} \quad (10)$$

Here T is the half-period of the particle, i.e. the time it takes for the particle to fall from its maximal radius to the minimal one

$$T(r_0, \mu) = \int_{r_{min}}^{r_0} \frac{dr}{v_r} \quad (11)$$

$T(r_0, \mu)$ is, generally speaking, a function of r_0 and μ .

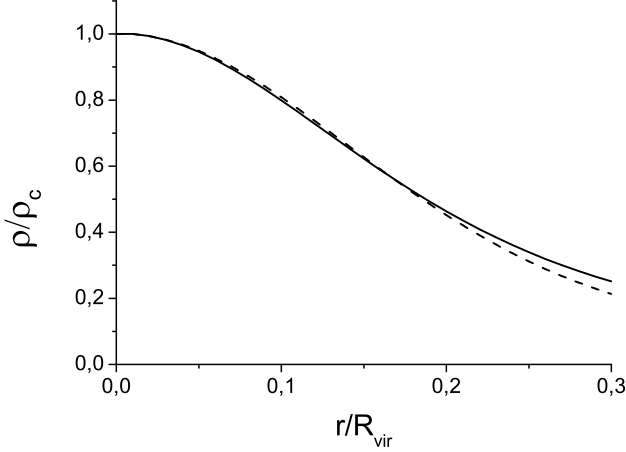


Figure 3. The density profile of the exact solution of (13) for $f(r_0) = M_{vir}\delta(r_0 - R_{vir})$ (dashed line) and profile (19) with the same r_c/R_{vir} (solid line). One can see that the departure of approximative equation (19) from the exact solution is quite small.

We can obtain the density distribution from (10), substituting there (9) instead of v_r and $4\pi r^2\rho$ instead of dm :

$$\rho = \frac{m}{4\pi r^2 v_r T} = \frac{mr_0}{4\pi r T \sqrt{r_0^2 - r^2} \sqrt{\mu_{max}^2 - \mu^2}} \quad (12)$$

In order to find the density distribution produced by all the particles of the halo with a certain r_0 (their total mass we have denoted by m), we should integrate (12) over distribution (6).

$$\rho = \frac{mr_0}{4\pi r \sqrt{r_0^2 - r^2}} \int_0^{\mu_{max}} \frac{2\mu \exp(-\mu^2/\alpha^2)}{\alpha^2 T(r_0, \mu) \sqrt{\mu_{max}^2 - \mu^2}} d\mu \quad (13)$$

This is the exact solution; we can significantly simplify it, however, if we take into account that $T(r_0, \mu)$ is in general a very weak function of μ , especially for small μ , since $T(r_0, \mu)$ has an extremum at $\mu = 0$. As we see in Fig. 2, $T(\mu)$ differs from $T(0)$ on no more, than 25%, for any reasonable potential, if $\mu \leq 0.5\mu_{circ}$, where μ_{circ} is the angular momentum corresponding to the circular orbit. Only particles with small μ can reach the central region under consideration: consequently, we may approximate T by $T(r_0) \equiv T(r_0, 0)$: Then we can take the integral in (13)

$$\rho = \frac{mr_0}{2\pi\alpha T(r_0)r\sqrt{r_0^2 - r^2}} D\left(\frac{\mu_{max}}{\alpha}\right) \quad (14)$$

where D is the Dawson function $D(x) \equiv e^{-x^2} \int_0^x e^{t^2} dt$. Of course, all particles in a real halo have some distribution over r_0 :

$$dm = f(r_0)dr_0 \quad (15)$$

In order to take it into account, we should substitute $f(r_0)dr_0$ instead of m to (14) and integrate the result over r_0 . Moreover, equation (14) can be significantly simplified in the central part of the halo. First of all, gravitational potential of the centre of the halo, $\phi(0)$, is finite for any reasonable halo profile (otherwise the annihilation signal, produced by the halo, would be infinite, being proportional

to $\int 4\pi r^2 \rho^2 dr$). Then we may rewrite (8) as

$$\mu_{max}^2 = 2r^2(\phi(r_0) - \phi(0)) \left(1 - \frac{\phi(r) - \phi(0)}{\phi(r_0) - \phi(0)}\right) \frac{r_0^2}{r_0^2 - r^2} \quad (16)$$

The two last factors may be neglected in the center of the halo, and we can use approximations $\mu_{max} \simeq r\sqrt{2(\phi(r_0) - \phi(0))}$, $\sqrt{r_0^2 - r^2} \simeq r_0$. So the total density distribution in the central part is

$$\rho = \int_0^\infty \frac{f(r_0)}{2\pi\alpha(r_0)T(r_0)r} D\left(\frac{r\sqrt{2(\phi(r_0) - \phi(0))}}{\alpha(r_0)}\right) dr_0 \quad (17)$$

Here we use designation $\alpha(r_0)$ instead of α in order to emphasize that α is, generally speaking, a function of r_0 .

As we could see, function $f(r_0)$ sharply depends on r_0 and differs noticeably from zero only on the interval between $\sim R_{vir}$ and $\sim R_{vir}/2$. On the contrary, $\alpha(r_0)$ should not change much on interval $[R_{vir}, R_{vir}/2]$: $\alpha(r_0)$ is widely believed to be a power-law dependence with the index between -1 and 1 (Hansen et al. 2006). $\sqrt{2(\phi(r_0) - \phi(0))}$ changes even slower: for instance, $\sqrt{(\phi(R_{vir}) - \phi(0))/(\phi(R_{vir}/2) - \phi(0))} \simeq 1.13$ for the NFW profile with $c_{vir} = 5$. Comparing this with the sharp behavior of $f(r_0)$, we may neglect the weak dependence of the argument of function D in (17) on r_0 and substitute there some value, averaged over the halo

$$r_c = \left\langle \frac{\alpha(r_0)}{\sqrt{2(\phi(r_0) - \phi(0))}} \right\rangle \simeq \frac{\langle \alpha(r_0) \rangle}{\sqrt{2|\phi(0)|}} \quad (18)$$

Then we can rewrite (17) and obtain the final result:

$$\rho = \rho_c \frac{r_c}{r} D\left(\frac{r}{r_c}\right), \quad \rho_c = \frac{1}{2\pi r_c} \int_0^\infty \frac{f(r_0)dr_0}{\alpha(r_0)T(r_0)} \quad (19)$$

Since $D(r/r_c) \simeq r/r_c$, when $r/r_c \rightarrow 0$, ρ_c is the central density of the halo. As we can see, it is always finite. At the same time, the shape of the density profile depends on the only parameter r_c .

4 DISCUSSION

Before proceeding any further, we should estimate the characteristic value of α . This question is, generally speaking, not quite clear. According to the modern cosmological conceptions, the initial angular momentum of each dark matter particle was very small (Gorbunov & Rubakov 2011), and it is the assumption that is routinely used in the N-body simulations. However, the particles can acquire some momentum in the subsequent relaxation. There are some grounds for believing that the mean-square-root angular momentum of the dark matter in the halo of the Milky Way, for instance, is small (Baushev 2011). A detailed consideration of this problem goes far beyond the scope of this letter. However, N-body simulations generally result in the mean-square-root angular momentum, close to the maximum possible one, and, as our consideration is oriented to the numerical calculations, we will proceed from this assumption and accept

$$\langle \alpha \rangle = \frac{1}{4} R_{vir} \sqrt{\frac{GM_{vir}}{R_{vir}}} = \frac{1}{4} \sqrt{GM_{vir} R_{vir}} \quad (20)$$

which roughly corresponds to the situation, when all particles with $r_0 = 0.75R_{vir}$ and $v < v_{esc}$ at this radius fall

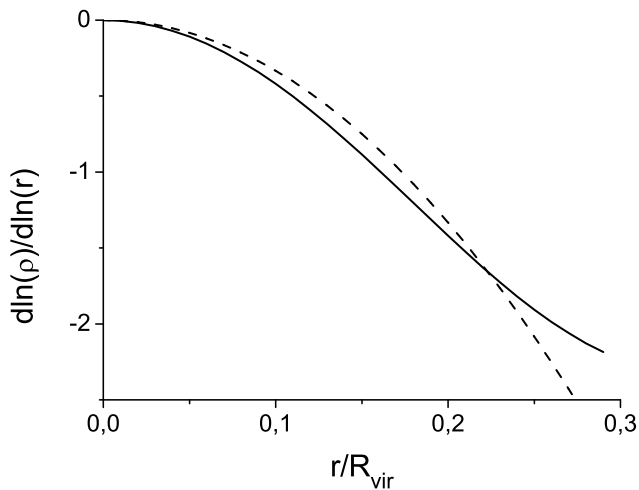


Figure 4. Density profile (19) of the central region of a halo with $r_c = R_{vir}/5.74$. Einasto profile with $n = 0.5$ and $r_s = 0.06R_{vir}$ is plotted for comparison (dashed line).

within the 3σ interval of distribution (6). It is apparent that $\langle \alpha \rangle$ cannot substantially exceed (20): otherwise a significant part of the dark matter would not be gravitationally bound in the halo.

In deriving (19) we used several times the fact that $r \ll r_0$. This raises the question: for what r/R_{vir} is equation (19) still valid? In order to check this, we solved numerically exact equation (13) on condition (6) and for distribution $f(r_0) = M_{vir}\delta(r_0 - R_{vir})$. $\phi(r)$ appears in expression (13), and we need to write out equation

$$\frac{d\phi}{dr} = \frac{G}{r^2} \int_0^r 4\pi x^2 \rho(x) dx$$

in order to close the task. The exact density profile (dashed line) and profile (19) with the same r_c/R_{vir} (solid line) are represented in Fig. 3. We see that (19) well approximates the exact solution up to $r \simeq 0.3R_{vir}$. So (19) can be valid in quite a large area around the halo centre.

Fig. 4 represents density profile (19) for $r_c = R_{vir}/5.74$. For reference, Einasto profile with $n = 0.5$ and $r_s = 0.06R_{vir}$ is also plotted. As we can see, the profiles are as a whole similar. However, (19) is steeper than the Einasto profile, and in this sense is closer to the Navarro-Frenk-White one. Taking into account large uncertainties of the N-body calculation results (Stadel et al. 2009), we may conclude that profile (19) is in excellent agreement with the simulations.

In conclusion, we would like to summarize the main conclusions of this letter. First, the density profile in the central part of a formed halo is really quite universal and weakly depends on the shape of the initial perturbation. This is a result of the fact that the potential well of the formed halo is much deeper than that of the initial perturbation. As a result, quite a large area builds up in the centre of the halo, where the particles do not reside, but just come there from the outside: their apoapses lie outside of the area. In order that the orbit of a particle entirely lie within the area, the particle energy should be dramatically decreased with respect to the initial value. Such a process is always hampered in a dissipationless system, and hence the particles, coming to the central area from the outside, dominate there and

form Einasto-like universal density profile (19). The shape of the profile is totally determined by single parameter r_c (18).

Second, the density in the centre of a halo should be finite even in the case, when the dark matter is cold. Indeed, one can see that equation (13) always asymptotically converges to (19) when $r \rightarrow 0$ (i.e., the central density remains finite), even if the angular momentum distribution completely differs from (6). There are only two possible situations, when this conclusion is incorrect, and the cusp formation is possible. It is feasible if angular momentum distribution (6) has a peculiarity at $\mu = 0$, i.e. the halo contains an anomalous number of particles with virtually zero angular momentum. This seems very unlikely. The cusp formation is also possible, if the halo contains a lot of particles with the energies, almost precisely equal to $\phi(0)$. The particles continuously reside in the centre of the halo and it is these particles that form the cusp. It is worthy of note, however, that the mass of the particles should be quite significant. In the case of Navarro-Frenk-White profile with $c_{vir} = 5 - 10$, for instance, the cusp area (with the profile, close to r^{-1}) comprises 13 – 20% of the total halo mass. As it has been already mentioned, the energy of the particles should be at least several times decreased with respect to the initial value, and so wide variations of such a large fraction of the halo particles are improbable. Moreover, as we discussed in the *energy spectrum* section, the parameters of the energy exchange process critically depend on the initial conditions, i.e. the form and even the existence of the cusp should be defined by the shape of the initial perturbation. N-body simulations indicate the opposite.

Third, contrary to the central part, the density profile of the halo outer regions essentially depends on the shape of distribution $f(r_0)$ (15). $f(r_0)$ is, in its turn, sensitive to the details of the relaxation process. Consequently, we may expect that the density profile of the outer regions of haloes ($r > 0.5R_{vir}$) is not universal and depends on the initial conditions to a degree.

Financial support by Bundesministerium für Bildung und Forschung through DESY-PT, grant 05A11IPA, is gratefully acknowledged. BMBF assumes no responsibility for the contents of this publication.

REFERENCES

- Baushev A. N., 2011, MNRAS, 417, L83
 Baushev A. N., 2012, MNRAS, 420, 590
 Diemand J., Kuhlen M., Madau P., Zemp M., Moore B., Potter D., Stadel J., 2008, Natur, 454, 735
 Gao L., Navarro J. F., Cole S., Frenk C. S., White S. D. M., Springel V., Jenkins A., Neto A. F., 2008, MNRAS, 387, 536
 Gorbunov, D. S., and Rubakov, V. A., 2011, *Introduction to the Theory of the Early Universe: Cosmological perturbations and inflationary theory*, World Scientific, Singapore.
 Einasto J., 1969, Astrofizika, 5, 137
 Hansen S. H., Moore B., Zemp M., Stadel J., 2006, JCAP, 1, 14
 Huss A., Jain B., Steinmetz M., 1999, ApJ, 517, 64
 Lithwick Y., Dalal N., 2011, ApJ, 734, 100

- Dalal N., Lithwick Y., Kuhlen M., 2010, arXiv, arXiv:1010.2539
- Lynden-Bell D., 1967, MNRAS, 136, 101
- Moore B., Lake G., Katz N., 1998, ApJ, 495, 139
- Navarro J. F., Frenk C. S., White S. D. M., 1997, ApJ, 490, 493
- Navarro J. F., Ludlow A., Springel V., et al., 2010, MNRAS, 402, 21
- Stadel J., Potter D., Moore B., Diemand J., Madau P., Zemp M., Kuhlen M., Quilis V., 2009, MNRAS, 398, L21
- Quinn P. J., Zurek W. H., 1988, ApJ, 331, 1
- Wang J., White S. D. M., 2009, MNRAS, 396, 709
- Zaroubi S., Naim A., Hoffman Y., 1996, ApJ, 457, 50